

# A METASTABLE SPIKE SOLUTION FOR A NON-LOCAL REACTION-DIFFUSION MODEL

David Iron and Michael J. Ward<sup>1</sup>

*Department of Mathematics, University of British Columbia  
Vancouver, B.C. V6T 1Z2, Canada*

## Abstract

An asymptotic reduction of the Gierer Meinhardt activator-inhibitor system in the limit of large inhibitor diffusivity leads to a singularly perturbed non-local reaction diffusion equation for the activator concentration. In the limit of small activator diffusivity, a one-spike solution to this non-local model is constructed. The spectrum of the eigenvalue problem associated with the linearization of the non-local model around such an isolated spike solution is studied in both a one-dimensional and a multi-dimensional context. It is shown that the principal eigenvalues in the spectrum are exponentially small in the limit of small activator diffusivity. The non-local term in the eigenvalue problem is essential for ensuring the existence of such exponentially small principal eigenvalues. These eigenvalues are responsible for the occurrence of an exponentially slow, or metastable, spike-layer motion for the time-dependent problem. Explicit metastable spike dynamics are derived by using a projection method, which enforces a limiting solvability condition on the solution to the linearized problem.

## 1 Introduction

In 1957 Turing proposed a mathematical model for morphogenesis, that describes the development of complex organisms from a single cell. He speculated that localized peaks in concentration of a chemical substance, known as an inducer or morphogen, could be responsible for a group of cells developing differently from the surrounding cells. He then demonstrated, with linear analysis, how a nonlinear reaction diffusion system could possibly generate such isolated peaks [14]. Later, Gierer and Meinhardt [4] demonstrated the existence of such solutions numerically for the following dimensionless reaction diffusion system

$$A_t = \epsilon^2 \Delta A - A + \frac{A^p}{H^q}, \quad \mathbf{x} \in \Omega, \quad t > 0 \quad (1a)$$

$$\tau H_t = D_h \Delta H - \mu H + \frac{A^m}{H^s} \quad \mathbf{x} \in \Omega, \quad t > 0 \quad (1b)$$

$$\partial_n A = 0, \quad \partial_n H = 0, \quad \mathbf{x} \in \partial\Omega. \quad (1c)$$

---

<sup>1</sup>This work was supported by NSERC grant 5-81541

Here  $\Omega$  is a closed bounded domain in  $\mathbb{R}^N$  and the exponents  $(p, q, m, s)$  satisfy

$$p > 1, \quad q > 0, \quad m > 0, \quad s \geq 0, \quad 0 < \frac{p-1}{q} < \frac{m}{s+1}. \quad (2)$$

This system was then used in [4] to model head formation in the *hydra*.

The numerical studies of [4] and more recently those of [6] have revealed that in the limit  $\epsilon \rightarrow 0$ , the activator concentration  $A$  for (1) can have localized regions of spatial extent  $O(\epsilon)$  where its concentration is elevated from a constant background concentration. Such solutions are called spike-type solutions. Some properties of spike-type equilibrium solutions have been obtained in [7], [10] and [13]. In this paper we will examine the dynamic motion of a one-spike solution to (1) in the limit  $D_h \rightarrow \infty$  and  $\epsilon \rightarrow 0$ . In this limit, (1) reduces to a non-local reaction diffusion model. Before we give an explicit outline of the paper we introduce an appropriate scaling of (1) for spike-type solutions and we derive the non-local reaction diffusion model corresponding to the limit  $D_h \rightarrow \infty$ .

The amplitude of a spike solution to (1) will tend to infinity as  $\epsilon \rightarrow 0$ . Therefore, we introduce new variables for which the spike solution has an  $O(1)$  amplitude as  $\epsilon \rightarrow 0$ . To this end, we introduce  $a$  and  $h$  by

$$A = \epsilon^{-\nu_a} a, \quad H = \epsilon^{-\nu_h} h, \quad (3)$$

where  $\nu_a$  and  $\nu_h$  are to be found. To balance the terms in (1a), we require,

$$-\nu_a = -\nu_a p + q \nu_h. \quad (4)$$

We will construct a solution in which the spike has its support in an  $O(\epsilon)$  region near some point in  $\Omega$ . Therefore, to obtain an additional equation relating  $\nu_a$  and  $\nu_h$  we consider an average balancing of (1b). Specifically, we integrate (1b) over the domain to get,

$$\tau \int_{\Omega} H_t d\mathbf{x} = -\mu \int_{\Omega} H d\mathbf{x} + \int_{\Omega} \frac{A^m}{H^s} d\mathbf{x}. \quad (5)$$

Since  $A$  will be localized to an  $O(\epsilon)$  region about the spike center  $\mathbf{x}_0$ , we scale  $\mathbf{x}$  in the last term by  $\mathbf{y} = \epsilon^{-1}(\mathbf{x} - \mathbf{x}_0)$ . Balancing the terms in this equation we get

$$-\nu_h = -\nu_a m + \nu_h s + N. \quad (6)$$

The solution of (4) and (6) yields,

$$\nu_a = \frac{Nq}{(1-p)(1+s) + mq}, \quad \nu_h = \frac{N(p-1)}{(1-p)(1+s) + mq}. \quad (7)$$

In terms of these new variables (1) becomes

$$a_t = \epsilon^2 \Delta a - a + \frac{a^p}{h^q}, \quad \text{in } \Omega, \quad t > 0 \quad (8a)$$

$$\tau h_t = D_h \Delta h - \mu h + \epsilon^{-N} \frac{a^m}{h^s}, \quad \text{in } \Omega, \quad t > 0 \quad (8b)$$

$$a_n = 0, \quad h_n = 0 \quad \text{on } \partial\Omega. \quad (8c)$$

Next we examine (8) in the limit  $D_h \rightarrow \infty$ . In this limit  $h$  will be a spatially constant to leading order, and hence the leading order equations for  $h$  and  $a$  will decouple, resulting in a non-local equation for  $a$ .

We begin by writing  $h$  as a power series in  $D_h^{-1}$ ,

$$h = h_0 + D_h^{-1}h_1 + \dots \quad (9)$$

Substituting (9) into (8), and collection powers of  $D_h^{-1}$  results in,

$$\Delta h_0 = 0, \quad \text{in } \Omega \quad (10a)$$

$$\Delta h_1 = \tau h_{0t} + \mu h_0 - \epsilon^{-N} \frac{a^m}{h_0^s}, \quad \text{in } \Omega, \quad (10b)$$

$$\partial_n h_0 = 0, \quad \text{on } \partial\Omega \quad (10c)$$

$$\partial_n h_1 = 0, \quad \text{on } \partial\Omega. \quad (10d)$$

Equations (10a) and (10c) imply that  $h_0$  is spatially homogeneous and thus  $h_0 = h_0(t)$ . Applying a solvability equation to (10b) using (10d) results in the following ordinary differential equation for  $h_0(t)$ ,

$$\tau \dot{h}_0 + \mu h_0 - \epsilon^{-N} \frac{1}{|\Omega|} \int_{\Omega} \frac{a^m}{h_0^s} d\mathbf{x} = 0. \quad (11)$$

Here  $\dot{h}_0 \equiv dh_0/dt$  and  $|\Omega|$  is the volume of  $\Omega$ . Typically  $\tau$  is small and thus the dynamics of  $h$  are much faster than that of  $a$ . So we set  $\dot{h}_0 = 0$  in (11) to obtain

$$h_0 = \left( \frac{\epsilon^{-N}}{\mu|\Omega|} \int_{\Omega} a^m d\mathbf{x} \right)^{\frac{1}{s+1}}. \quad (12)$$

In the analysis below, we will only be considering the leading order term of  $h$ . Thus, we label  $h_0$  by  $h$ . Substituting the value of  $h$  into (8) results in the following scalar non-local reaction diffusion equation;

$$a_t = \epsilon^2 \Delta a - a + \frac{a^p}{h^q}, \quad \text{in } \Omega, \quad t > 0, \quad (13a)$$

$$h = \left( \frac{\epsilon^{-N}}{\mu|\Omega|} \int_{\Omega} a^m d\mathbf{x} \right)^{\frac{1}{s+1}}, \quad (13b)$$

$$\partial_n a = 0 \quad \text{on } \partial\Omega. \quad (13c)$$

This system, referred to as the *Shadow System* [11], is studied below. It will also be studied in a one-dimensional domain  $x \in [-1, 1]$ . In this case, (13) reduces to

$$a_t = \epsilon^2 a_{xx} - a + \frac{a^p}{h^q}, \quad -1 < x < 1, \quad t > 0, \quad (14a)$$

$$h = \left( \frac{\epsilon^{-1}}{2\mu} \int_{-1}^1 a^m dx \right)^{\frac{1}{s+1}}, \quad (14b)$$

$$a_x(\pm 1, t) = 0. \quad (14c)$$

The outline of the paper is as follows. In §2 we consider the one-dimensional problem (14). In this case, we construct a one-spike quasi-equilibrium solution. We examine the stability and dynamics of this solution by analyzing the spectrum of the linear operator resulting from a linearization of (14) about this non-constant solution. This eigenvalue problem is a non-local Sturm-Liouville problem of the type considered in [3]. A combination of analytical and numerical techniques will be used to demonstrate that the principle eigenvalue of this operator is exponentially small. The non-local term is essential for this conclusion. The exponentially small eigenvalue will be estimated asymptotically. A differential equation characterizing the motion of the center of the spike will be derived in the limit  $\epsilon \rightarrow 0$  by using a limiting solvability condition, which requires that the solution to the quasi-steady linearized problem has no component in the eigenspace associated with the exponentially small eigenvalue. This procedure is known as the projection method and has been used in other contexts (see [15], [16], [17]). The resulting ODE for the motion of the center of the spike, shows that the spike drifts exponentially slowly towards the point on the boundary closest to the initial location of the spike. This metastable behavior is verified by calculating full numerical solutions to (14). In §3 we give a similar analysis of metastable spike-layer motion for the multi-dimensional problem (13).

## 2 A Spike in a One-Dimensional Domain

We first construct a one-spike quasi-equilibrium solution  $a_E$  for (14) in the form

$$a = a_E(x; x_0) \equiv h^\gamma u_c[\epsilon^{-1}(x - x_0)], \quad \gamma = q/(p-1). \quad (15)$$

Here  $x_0$ , with  $|x_0| < 1$ , is the center of the spike. The function  $u_c(y)$ , called the canonical spike solution, satisfies

$$u_c'' - u_c + u_c^p = 0, \quad 0 < y < \infty, \quad (16a)$$

$$u_c'(0) = 0; \quad u_c(y) \sim ae^{-y}, \quad \text{as } y \rightarrow \infty. \quad (16b)$$

It is easily seen from phase plane considerations that such a solution exists. In terms of this solution,  $h = h_E$ , where

$$h_E = \left( \frac{1}{2\epsilon\mu} \int_{-1}^1 u_c^m dx \right)^{\frac{p-1}{(s+1)(p-1)-qm}}. \quad (17)$$

Since  $u_c$  is localized near  $x_0$ , we estimate

$$h_E \sim \left( \frac{\beta}{\mu} \right)^{\frac{p-1}{(s+1)(p-1)-qm}}, \quad \beta \equiv \int_0^\infty [u_c(y)]^m dy. \quad (18)$$

To determine numerical values for certain asymptotic quantities below we must compute  $u_c(y)$ ,  $\beta$ , and  $a$  numerically. The constant  $a$  is obtained by

integrating (16)

$$\log(a) = \frac{\log\left(\frac{p+1}{2}\right)}{p-1} + \int_0^{\left(\frac{p+1}{2}\right)^{\frac{1}{p-1}}} \left[ \frac{-1}{\sqrt{\eta^2 - \frac{2}{p+1}\eta^{p+1}}} - \frac{1}{\eta} \right] d\eta. \quad (19)$$

To compute  $u_c$  numerically, we use the asymptotic boundary condition  $u_c' + u_c = 0$  at  $y = y_L$ , where  $y_L$  is a large positive constant. To compute solutions for various values of  $p$ , we use a continuation procedure starting from the special analytical solution,

$$u_c(y) = \frac{3}{2} \operatorname{sech}^2\left(\frac{y}{2}\right), \quad (20)$$

which holds when  $p = 2$ . The boundary value solver COLNEW (see [1]) is then used to solve the resulting boundary value problem. In Fig. 1, we plot the numerically computed  $u_c(y)$  when  $p = 2, 3, 4$ .

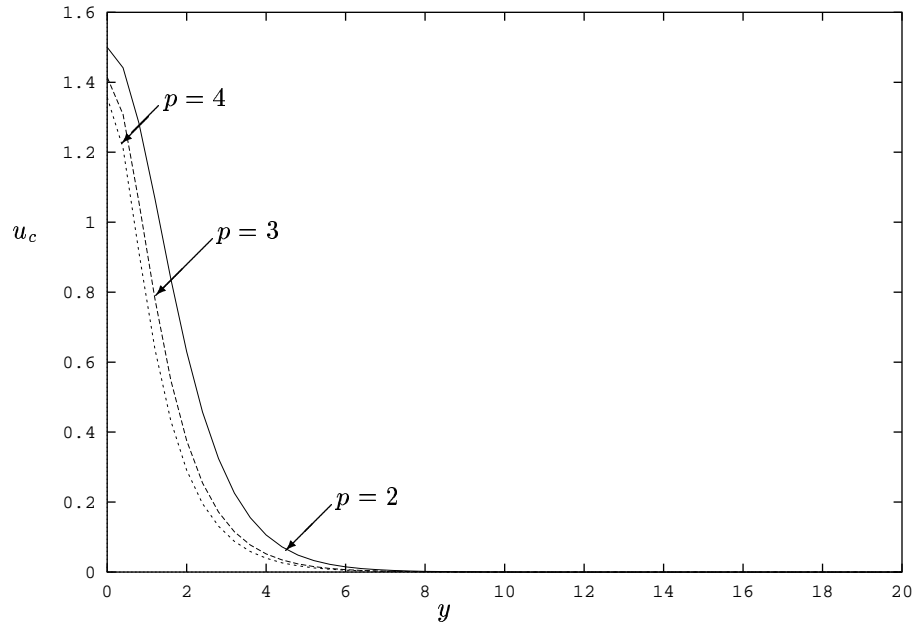


Figure 1: Numerical solution for  $u_c(y)$  when  $p = 2, 3, 4$ .

We note that, for any  $x_0$  with  $|x_0| < 1$ , the solution  $a_E(x; x_0)$  will satisfy the steady-state problem corresponding to (14a), but will fail to satisfy the boundary

conditions in (14c) by only exponentially small terms as  $\epsilon \rightarrow 0$ . Thus, we expect that the spectrum of the eigenvalue problem associated with the linearization about  $a_E$  will contain an exponentially small eigenvalue.

## 2.1 The Nonlocal Eigenvalue Problem

Let  $x_0 \in (-1, 1)$  be fixed and linearize (14) around  $a_E$ ,  $h_E$ . We obtain the eigenvalue problem for the linearization by introducing  $\phi$  and  $\eta$  by

$$a(x, t) = a_E(x; x_0) + e^{\lambda t} \phi \quad (21a)$$

$$h(t) = h_E + e^{\lambda t} \eta, \quad (21b)$$

$$(21c)$$

where  $\phi \ll 1$  and  $\eta \ll 1$ . Substituting (21) into (14) we obtain the following non-local eigenvalue problem of Sturm-Liouville type on  $[-1, 1]$ :

$$L_\epsilon \phi \equiv \epsilon^2 \phi_{xx} + (-1 + pu_c^{p-1})\phi - \frac{mq\epsilon^{-1}u_c^p}{2\beta(s+1)} \int_{-1}^1 u_c^{m-1} \phi dx = \lambda \phi, \quad (22a)$$

$$\phi_x(\pm 1) = 0. \quad (22b)$$

The non-local integral term in (22) will drastically change the nature of the eigenvalue problem.

In (22),  $u_c = u_c[\epsilon^{-1}(x - x_0)]$ . Therefore, we will only seek eigenfunctions that are localized near  $x = x_0$ . These eigenfunctions are of the form

$$\tilde{\phi}(y) = \phi(x_0 + \epsilon y), \quad y = \epsilon^{-1}(x - x_0). \quad (23)$$

Therefore, we can replace the finite interval by an infinite interval in the integral in (22) and impose a decay condition for  $\tilde{\phi}(y)$  as  $y \rightarrow \pm\infty$ . This gives us the non-local eigenvalue problem for the infinite domain  $-\infty < y < \infty$ :

$$\tilde{L}_\epsilon \tilde{\phi} \equiv \tilde{\phi}_{yy} + (-1 + pu_c^{p-1})\tilde{\phi} - \frac{mqu_c^p}{2\beta(s+1)} \int_{-\infty}^{\infty} u_c^{m-1} \tilde{\phi} dy = \lambda \tilde{\phi}, \quad (24a)$$

$$\tilde{\phi} \rightarrow 0 \quad \text{as} \quad y \rightarrow \pm\infty. \quad (24b)$$

To treat the non-local eigenvalue problem, we split the operator  $L_\epsilon$  into two parts,

$$A\phi \equiv \epsilon^2 \phi_{xx} + (-1 + pu_c^{p-1})\phi, \quad B\phi \equiv \frac{mq\epsilon^{-1}u_c^p}{2\beta(s+1)} \int_{-1}^1 u_c^{m-1} \phi dx. \quad (25)$$

We define a new operator  $L_\delta$  by  $L_\delta \phi \equiv A\phi - \delta B\phi$ . where  $\delta$ , with  $0 < \delta < 1$ , is a continuation parameter. When  $\delta = 0$  we have a simple Sturm-Liouville problem. At  $\delta = 1$  we have our full non-local eigenvalue problem (22). We define  $\tilde{L}_\delta$ ,  $\tilde{A}$  and  $\tilde{B}$  in a similar fashion, but on the extended domain  $-\infty < y < \infty$  with the appropriate boundary conditions at  $\pm\infty$ .

The operator  $\tilde{L}_\epsilon$  has a zero eigenvalue with eigenfunction  $u'_c$ , which decays exponentially as  $|y| \rightarrow \infty$ . To see this, we differentiate (16a) with respect to  $y$ , to show that  $\tilde{A}u'_c = 0$ . This is translation invariance. In addition, due to the symmetry of  $u_c(y)$ , we also have  $\tilde{B}u'_c = 0$ . For the finite domain problem (22), the function  $u_c[\epsilon^{-1}(x - x_0)]$  fails to satisfy the equation and boundary conditions in (22) by only exponentially small terms as  $\epsilon \rightarrow 0$ . Therefore, as estimated carefully below, the presence of the finite domain will perturb the zero eigenvalue and corresponding eigenfunction of the extended problem (24) by only an exponentially small amount. Thus,  $L_\epsilon$  has an exponentially small eigenvalue.

The function  $u_c(y)$  has a unique maximum at  $y = 0$  and thus the eigenfunction  $u'_c(y)$  has exactly one zero at  $y = 0$ . This implies that  $u'_c(y)$  corresponds to the second eigenfunction of  $\tilde{A}$ . The principal eigenvalue of  $\tilde{A}$  is simple, positive and independent of  $\epsilon$ . The principal eigenvalue of  $A$  is exponentially close to the principal eigenvalue of  $\tilde{A}$ . Hence, in the absence of the non-local term, the operator  $L_\epsilon$  has an  $O(1)$  positive eigenvalue and no metastable spike motion can occur.

Since  $\tilde{L}_\delta$  has a positive eigenvalue when  $\delta = 0$ , we must consider what happens to this eigenvalue as  $\delta$  ranges from 0 to 1. If this eigenvalue remains positive then, since the eigenvalues of  $L_\delta$  and  $\tilde{L}_\delta$  will differ by only exponentially small amounts as  $\epsilon \rightarrow 0$ , we can conclude that the one-spike quasi-equilibrium solution is unstable. Alternatively, if this eigenvalue crosses through zero at some finite value of  $\delta < 1$ , then the principal eigenvalue of  $L_\delta$  when  $\delta = 1$  (which corresponds to our eigenvalue problem (22)) will be exponentially small. Hence, if this occurs, the one-spike solution is anticipated to be metastable.

The calculation of the eigenvalues of  $\tilde{L}_\delta$  will require some numerical analysis. Thus, we will work with specific parameter sets. We first consider the set  $(p, q, m, s) = (2, 1, 2, 0)$ , which are commonly used in simulations. For this parameter set, we begin by reviewing some exact results for the spectrum of the local eigenvalue problem

$$\tilde{A}\tilde{\phi} \equiv \tilde{\phi}_{yy} + (-1 + pu_c^{p-1})\tilde{\phi} = \lambda\tilde{\phi} \quad -\infty < y < \infty, \quad (26a)$$

$$\tilde{\phi} \rightarrow 0 \quad \text{as} \quad y \rightarrow \pm\infty. \quad (26b)$$

This problem has three isolated eigenvalues and a continuous spectrum. When  $p = 2$ , these three isolated eigenpairs are (see [8]),

$$\lambda_0 = 5/4, \quad \tilde{\phi}_0 = \text{sech}^3(y/2), \quad (27)$$

$$\lambda_1 = 0, \quad \tilde{\phi}_1 = \tanh(y/2)\text{sech}^2(y/2), \quad (28)$$

$$\lambda_2 = -3/4, \quad \tilde{\phi}_2 = 5\text{sech}^3(y/2) - 4\text{sech}(y/2). \quad (29)$$

Since these eigenfunctions, written in terms of  $y = \epsilon^{-1}(x - x_0)$ , will fail to satisfy the boundary conditions in (22) by only exponentially small terms as  $\epsilon \rightarrow 0$ , we expect that the eigenvalues of  $A$  will be only slightly perturbed from those of  $\tilde{A}$ . As we have previously noted, the zero eigenvalue of (26) will persist for  $\tilde{L}_\delta$  as  $\delta$  ranges from zero to one. Hence, there is an eigenvalue of (22) that is exponentially small as  $\epsilon \rightarrow 0$ .

To numerically compute the eigenvalue branches  $\lambda_0(\delta)$  and  $\lambda_2(\delta)$  of  $\tilde{L}_\delta$  for which  $\lambda_0(\delta) \rightarrow 5/4$  and  $\lambda_2(\delta) \rightarrow -3/4$ , as  $\delta \rightarrow 0$ , we use the initial guesses provided above for  $\delta = 0$  and a continuation procedure to compute these eigenvalues as  $\delta$  increases. The computations are done using COLNEW. The analysis of [3] showed that these eigenvalue branches are smooth functions of  $\delta$ , which cannot terminate suddenly at some value of  $\delta$ . Hence,  $\delta$  is a natural homotopy parameter. In Fig. 2 we plot the numerically computed  $\lambda_0(\delta)$  and  $\lambda_2(\delta)$  versus  $\delta$ . As can be seen from this graph,  $\lambda_0 \approx 0$  for  $\delta = 1/2$ . As  $\delta$  increases past  $1/2$ ,  $\lambda_0$  becomes negative and then complex. At this point, COLNEW is no longer able to track the eigenvalue. As  $\delta$  increases from 0 to 1,  $\lambda_0$  is decreasing and  $\lambda_2$  is increasing. At a value of  $\delta \approx 0.65$  the two eigenvalues collide and split into complex conjugates eigenvalues with negative real parts. To track the eigenvalues beyond  $\delta \approx 0.65$  one must employ a different numerical technique. We accomplish this by discretizing the finite domain problem (22), which has eigenvalues exponentially close to those of  $\tilde{L}_\delta$ . This is done using a centered difference approximation applied to the second derivative and Simpson's rule applied to the integral. Thus, the operator  $L_\delta$  is approximated by a discrete linear operator  $\mathcal{L}_\delta$ . The eigenvalues of the continuous problem may then be approximated by the eigenvalues of this matrix. Numerical calculations of the eigenvalue  $\lambda_0$  of  $\mathcal{L}_\delta$  are shown in Table 1. Since the real part of  $\lambda_0$  remains negative as  $\delta \rightarrow 1$ , we conclude that the one-spike quasi-equilibrium solution is stable for this parameter set. Similar computations, with similar conclusions, can be performed for other values of  $p$ ,  $q$ ,  $m$  and  $s$ . In particular,  $\lambda_0$  and  $\lambda_2$  are shown in Fig. 3 for the parameter set  $(p, q, m, s) = (3, 2, 2, 0)$ .

$\delta$	$\lambda_0$
0.0	1.2518
0.1	1.0073
0.2	0.76149
0.3	0.51345
0.4	0.26158
0.5	0.0052548
0.6	-0.28247
0.7	$-.59237 + 0.15315i$
0.8	$-.71522 + 0.23035i$
0.9	$-.84093 + 0.23008i$
1.0	$-.98551 + 0.14507i$

Table 1:  $\delta$  and  $\lambda_0$  for the case  $(p, q, m, s) = (2, 1, 2, 0)$ .

## 2.2 An Exponentially Small Eigenvalue

In the previous section, we showed that the principal eigenvalue of  $L_\epsilon$  is exponentially small. The non-local term in (22) was found to be essential to

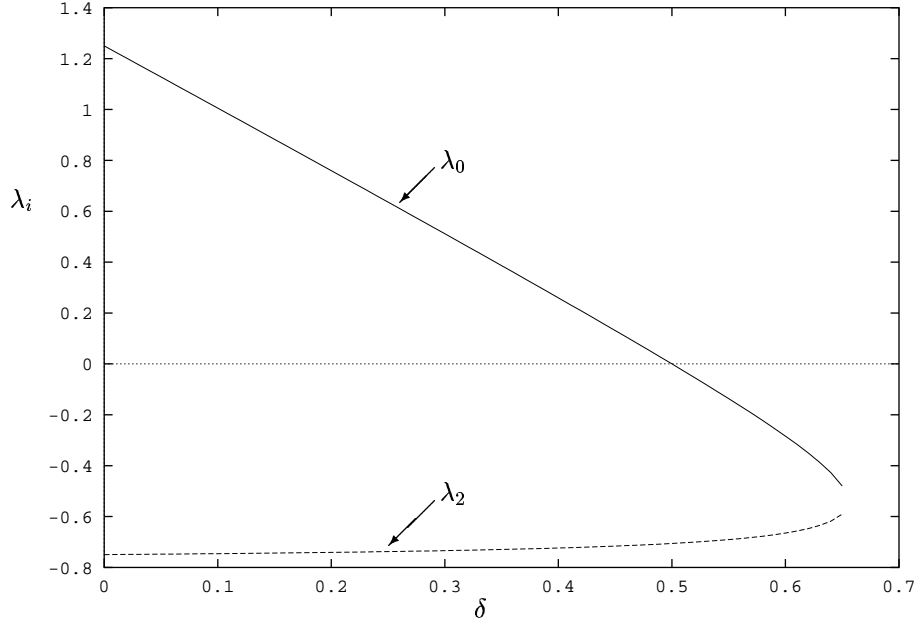


Figure 2:  $\lambda_0$  and  $\lambda_2$  versus  $\delta$  for the parameter set  $(p, q, m, s) = (2, 1, 2, 0)$ .

this conclusion. We denote the eigenpair corresponding to the exponentially small eigenvalue by  $\lambda_1, \phi_1$ . To predict the dynamics of the quasi-equilibrium solution, we must obtain a very accurate estimate of  $\lambda_1$ . We expect that  $\phi_1 \sim C_1 u'_c(\epsilon^{-1}(x - x_0))$  in the outer region away from  $O(\epsilon)$  boundary layers near  $x = \pm 1$ . The behavior of  $\phi_1$  in these regions will be analyzed using a boundary layer analysis.

The eigenfunction  $\phi_1$  has the boundary layer form

$$\phi_1(x) = C_1 (u'_c[\epsilon^{-1}(x - x_0)] + \phi_l[\epsilon^{-1}(x + 1)] + \phi_r[\epsilon^{-1}(1 - x)]) . \quad (30)$$

Here  $\phi_l(\eta)$  and  $\phi_r(\eta)$  are boundary layer correction terms and  $C_1$  is a normalization constant given by

$$C_1 = (\epsilon \hat{\beta})^{-1/2}, \quad \text{where } \hat{\beta} = \int_{-\infty}^{\infty} [u'_c(y)]^2 dy . \quad (31)$$

In the boundary layer region near  $x = -1$ ,  $u'_c[\epsilon^{-1}(x - x_0)]$  is exponentially

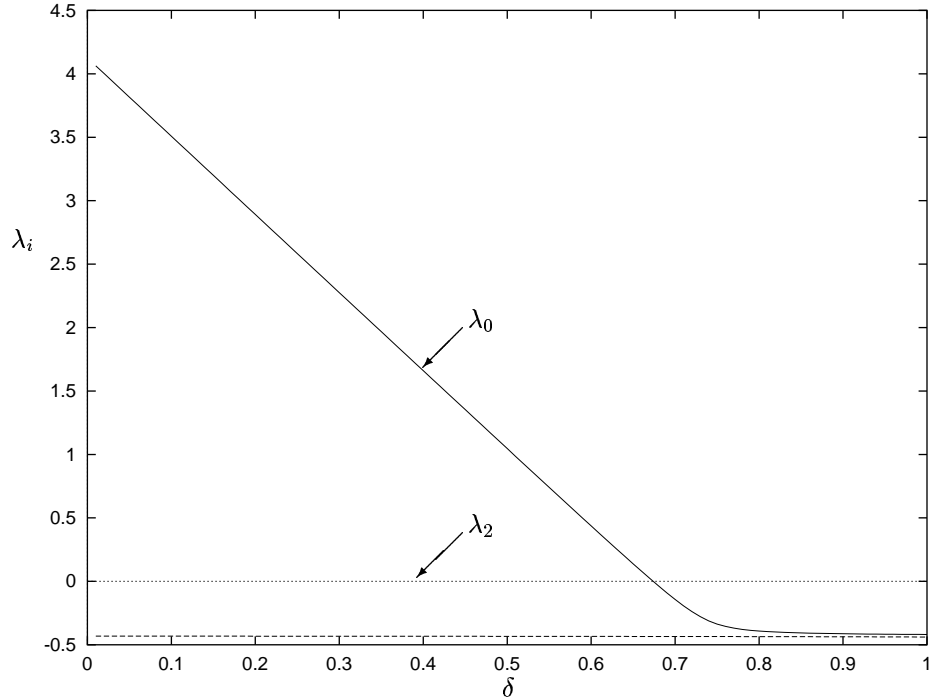


Figure 3:  $\lambda_0$  and  $\lambda_2$  versus  $\delta$  for the parameter set  $(p, q, m, s) = (3, 2, 2, 0)$ .

small as  $\epsilon \rightarrow 0$ . Thus, as  $\epsilon \rightarrow 0$ ,  $\phi_l(\eta)$  satisfies

$$\phi_l'' - \phi_l = 0, \quad 0 \leq \eta < \infty, \quad (32a)$$

$$\phi_l'(0) \sim -ae^{-\epsilon^{-1}(1+x_0)}. \quad (32b)$$

Similarly, the boundary layer equation for  $\phi_r(\eta)$  is

$$\phi_r'' - \phi_r = 0, \quad 0 \leq \eta < \infty, \quad (33a)$$

$$\phi_r'(0) \sim ae^{-\epsilon^{-1}(1-x_0)}. \quad (33b)$$

Here  $a$  is defined in (19). Solving the boundary layer equations we get

$$\phi_l(\eta) = ae^{-\epsilon^{-1}(1+x_0)}e^{-\eta}, \quad (34a)$$

$$\phi_r(\eta) = -ae^{-\epsilon^{-1}(1-x_0)}e^{-\eta}. \quad (34b)$$

To estimate  $\lambda_1$  we first derive Lagrange's identity for  $(u, L_\epsilon v)$ , where  $(u, v) \equiv$

$\int_{-1}^1 uv \, dx$ . Using integration by parts we derive

$$(v, L_\epsilon u) = \epsilon^2 (u_x v - v_x u) \Big|_{-1}^1 + (u, L_\epsilon^* v), \quad (35)$$

where

$$L_\epsilon^* v \equiv \epsilon^2 v_{xx} + (-1 + pu_c^{p-1})v - \frac{mq\epsilon^{-1}u_c^{m-1}}{2\beta(s+1)} \int_{-1}^1 u_c^p v \, dx. \quad (36)$$

We now apply this identity to the functions  $u'_c[\epsilon^{-1}(x - x_0)]$  and  $\phi_1(x)$  to get

$$\lambda_1(u'_c, \phi_1) = -\epsilon\phi_1 u_c'' \Big|_{-1}^1 + (\phi_1, L_\epsilon^* u'_c). \quad (37)$$

We examine each of the terms in (37). We begin with  $(u'_c, \phi_1)$ . The dominant contribution to this integral arises from the region near  $x = x_0$  where  $\phi_1 \sim C_1 u'_c[\epsilon^{-1}(x - x_0)]$ . Therefore, the inner product can be estimated as

$$(u'_c, \phi_1) = C_1(u'_c, u'_c) \sim C_1 \epsilon \hat{\beta}. \quad (38)$$

Next, to estimate  $-\epsilon\phi_1 u_c'' \Big|_{-1}^1$ , we use our asymptotic estimates of  $u_c$  and  $\phi_1$ . Since  $u_c(z) \sim ae^{-|z|}$  as  $z \rightarrow \pm\infty$  we have that  $u_c''[\epsilon^{-1}(\pm 1 - x_0)] \sim ae^{-\epsilon^{-1}(1 \mp x_0)}$ . In addition, using the previous boundary layer results for  $\phi_1$  we get the following estimate for  $\phi_1(\pm 1)$ :

$$\phi_1(\pm 1) \sim \mp 2C_1 a e^{-\epsilon^{-1}(1 \mp x_0)}. \quad (39)$$

Using these results, we get

$$-\epsilon\phi_1 u_c'' \Big|_{-1}^1 \sim 2\epsilon C_1 a^2 \left( e^{-2\epsilon^{-1}(1+x_0)} + e^{-2\epsilon^{-1}(1-x_0)} \right). \quad (40)$$

The only term left to examine is  $(\phi_1, L_\epsilon^* u'_c)$ . Since  $u'_c$  is a solution to the local operator, we have

$$\begin{aligned} L_\epsilon^* u'_c &= -\frac{mq\epsilon^{-1}u_c^{m-1}}{2\beta(s+1)} \int_{-1}^1 u_c^p u'_c \, dx, \\ &\sim -\frac{mq\epsilon^{-1}a^{p+1}u_c^{m-1}}{2\beta(s+1)(p+1)} \left( e_+^{p+1} - e_-^{p+1} \right), \end{aligned} \quad (41)$$

where

$$e_\pm^p \equiv e^{-p\epsilon^{-1}(1 \pm x_0)}. \quad (42)$$

In a similar way, the term  $(\phi_1, L_\epsilon^* u'_c)$  is approximated by

$$\begin{aligned} (\phi_1, L_\epsilon^* u'_c) &\sim -\frac{mq\epsilon^{-1}a^{p+1}C_1}{2\beta(s+1)(p+1)} \left( e_+^{p+1} - e_-^{p+1} \right) \int_{-1}^1 u_c^{m-1} u'_c \, dx, \\ &\sim -\frac{mq\epsilon^{-1}a^{p+m+1}C_1}{2\beta(s+1)(p+1)m} \left( e_+^{p+1} - e_-^{p+1} \right) (e_+^m - e_-^m). \end{aligned} \quad (43)$$

Since  $p > 1$  and  $m > 0$ , upon comparing the terms in (43) and (40), it is clear that the second term on the right side of (37) is asymptotically negligible compared to the first term. Finally, substituting (38) and (40) into (37), we get the following asymptotic estimate for the exponentially small eigenvalue  $\lambda_1$  as  $\epsilon \rightarrow 0$ :

$$\lambda_1 \sim 2a^2 \hat{\beta}^{-1} \left( e^{-2\epsilon^{-1}(1+x_0)} + e^{-2\epsilon^{-1}(1-x_0)} \right). \quad (44)$$

In (44),  $a$  and  $\hat{\beta}$  are defined in (19) and (31), respectively. The estimate (44) holds for  $p, q, m$  and  $s$  satisfying (2). Since  $\lambda_1 > 0$  but is exponentially small, we conclude that, although the spike solution is unstable, it may persist for extremely long times.

To verify the estimate for  $\lambda_1$ , we also numerically estimate  $\lambda_1$  by solving (22) using COLNEW. In Fig. 4, we compare the numerically computed values of  $\lambda_1$  (the dots) with the asymptotic estimate (44) (dashed curve) for various values of  $\epsilon$  for the parameter set  $(p, q, m, s) = (2, 1, 2, 0)$ . Similar favorable comparisons can be made for other parameter sets.

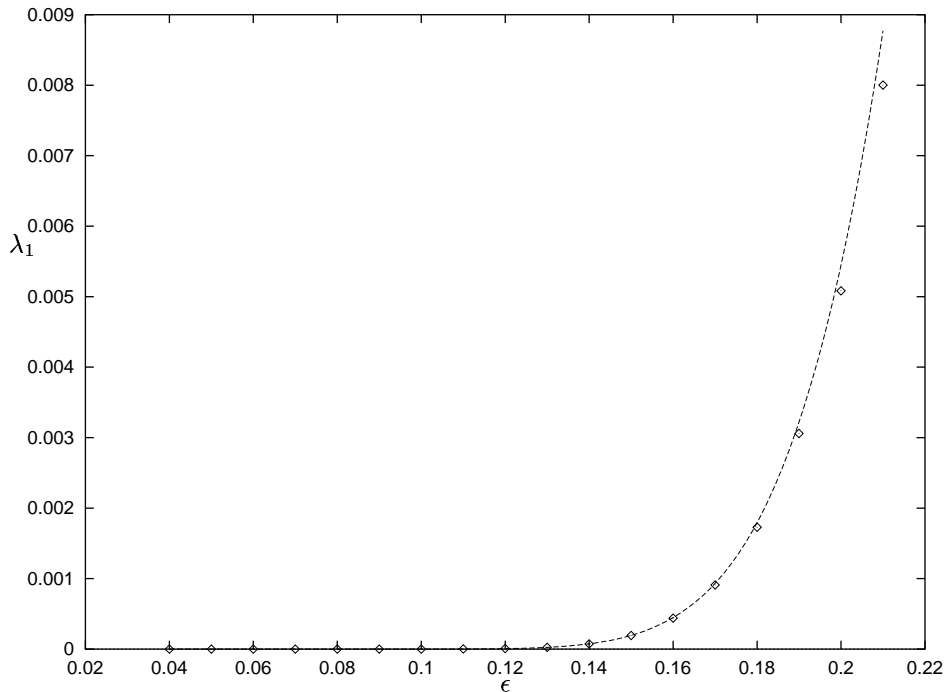


Figure 4:  $\lambda_1$  versus  $\epsilon$  for the parameter set  $(p, q, m, s) = (2, 1, 2, 0)$ .

We end this section with a few remarks. Firstly, we recall that  $\lambda_1$  and  $\phi_1 \sim C_1 u_c'(\epsilon^{-1}(x - x_0))$  are an eigenpair of  $L_\delta$  when  $\delta = 0$ . To within negligible exponentially small terms this eigenpair remains an eigenpair of  $L_\delta$  as  $\delta$  ranges from 0 to 1. To see this, we note that the only difference between the calculations of the eigenvalue for the local problem and for the non-local problem, is that the term  $(L_\epsilon^* u_c', \phi_1)$  in (37) would be replaced by  $(A\phi_1, \phi_1) = 0$ , since  $A$  is self-adjoint. In the final calculation of  $\lambda_1$  the term  $(L_\epsilon^* u_c', \phi_1)$  was ignored since it is asymptotically exponentially smaller than the other terms in (37). Secondly, we note that  $\lambda_1, \phi_1$  is exponentially close to an eigenpair  $\lambda_1^*, \phi_1^*$  of the adjoint operator,  $L_\epsilon^*$ . For the same reasoning as above,  $\phi_1^*$  would have the same interior behavior near  $x = x_0$  as  $\phi_1$  and the same boundary layer correction terms near  $x = \pm 1$ . Repeating the calculation to find  $\lambda_1^*$ , we would arrive at the same estimate as in (44).

### 2.3 The Slow Motion of the Spike

The quasi-equilibrium solution fails to satisfy the steady-state problem corresponding to (14) by only exponentially small terms for any value of  $x_0$  in  $|x_0| < 1$ . Moreover, the linearization about this solution admits a principal eigenvalue that is exponentially small. Therefore, we expect that the one-spike quasi-equilibrium solution evolves on an exponentially slow time-scale. We will now derive an equation of motion for the center of the spike corresponding to the quasi-equilibrium solution. To do so we first linearize (14) about  $a(x, t) = h^\gamma u_c[\epsilon^{-1}(x - x_0(t))]$ , where the spike location  $x_0 = x_0(t)$  is to be determined. For a fixed  $x_0$  we have shown that the linearization around this solution has an exponentially small principal eigenvalue as  $\epsilon \rightarrow 0$ . By eliminating the projection of the solution on the eigenfunction corresponding to this eigenvalue, we will derive an equation of motion for  $x_0(t)$ .

We begin by linearizing around a moving spike solution by writing,

$$a(x, t) = a_E(x; x_0(t)) + w(x, t) \quad (45)$$

where  $a_E$  is defined in (15) and  $x_0(t)$  is the trajectory of the spike. Since (22) does not have an  $O(1)$  positive eigenvalue, we may assume that  $w \ll a_E$  and  $w_t \ll \partial_t a_E$ . Substituting (45) into (14), we get

$$L_\epsilon w = \partial_t a_E, \quad -1 < x < 1, \quad t \geq 0 \quad (46a)$$

$$w_x(\pm 1, t) = -\partial_x a_E(\pm 1; x_0). \quad (46b)$$

Next, we expand  $w$  in terms of the eigenfunctions  $\phi_i$  of  $L_\epsilon$  as

$$w = \sum_{i=1}^{\infty} D_i(t) \phi_i. \quad (47)$$

The solvability condition for  $w$  is that  $w$  is orthogonal to the eigenspace of  $L_\epsilon^*$  associated with the exponentially small eigenvalue. Let  $\phi_i^*$  be the  $i^{\text{th}}$  eigenfunc-

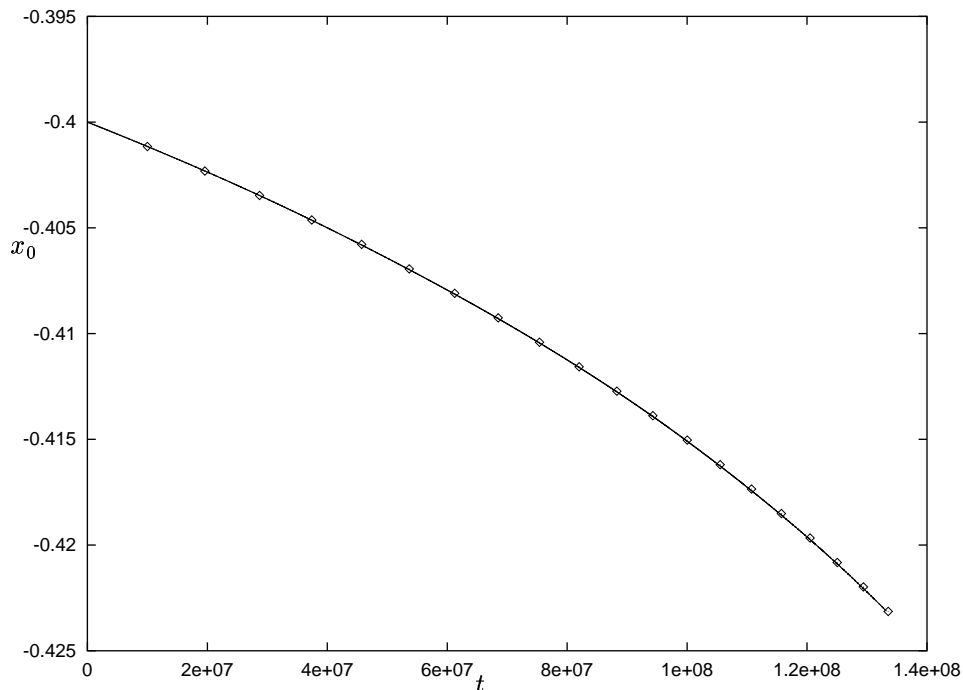


Figure 5:  $x_0$  versus  $t$  for  $\epsilon = .05$

tion of  $L_\epsilon^*$ . Then, since  $(\phi_i, \phi_j^*) = \delta_{ij}$ , we integrate by parts to show that

$$D_i(t) = (w, \phi_i^*) = \frac{1}{\lambda_i^*} [(L_\epsilon w, \phi_i^*) - \epsilon^2 w_x \phi_i^*|_{-1}^1], \quad (48)$$

where  $L_\epsilon^* \phi_i^* = \lambda_i^* \phi_i^*$ . Using (46), we have

$$D_i(t) = \frac{1}{\lambda_i^*} [(\partial_t a_E, \phi_i^*) + \epsilon^2 \phi_i^* \partial_x a_E|_{-1}^1]. \quad (49)$$

As discussed previously, when  $\epsilon \ll 1$ , the nonlocal term in the eigenvalue problem (22) is insignificant in asymptotic estimation of the eigenspace associated with the exponentially small eigenvalue of  $L_\epsilon$ . Therefore, we can replace  $\phi_1^*$  and  $\lambda_1^*$  by  $\phi_1$  and  $\lambda_1$  in (49), where  $\phi_1$  and  $\lambda_1$  are given in (30) and (44), respectively.

Since  $\lambda_1 \rightarrow 0$  exponentially as  $\epsilon \rightarrow 0$ , we must impose the limiting solvability condition that  $D_1 = 0$ . This projection step yields the following implicit differential equation for  $x_0(t)$ :

$$(\partial_t a_E, \phi_1) = -\epsilon^2 \phi_1 \partial_x a_E|_{-1}^1. \quad (50)$$

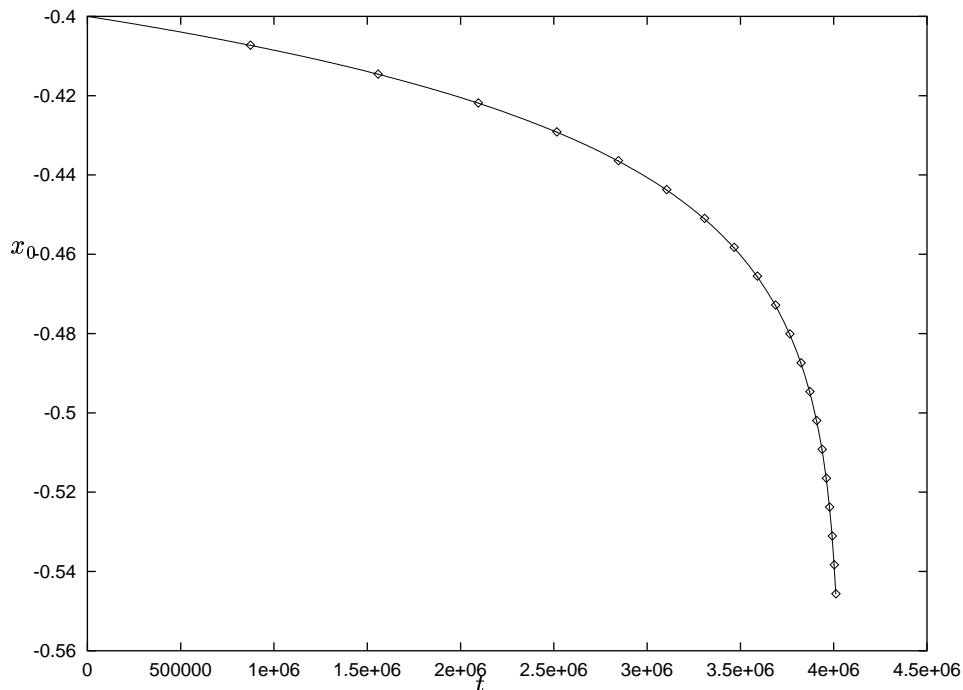


Figure 6:  $x_0$  versus  $t$  for  $\epsilon = .06$

The dominant contribution to the left side of (50) arises from the region near  $x_0$ . For  $\epsilon \rightarrow 0$ , we calculate

$$(\partial_t a_E, \phi_1) \sim -C_1 h_E^\gamma \dot{x}_0 \hat{\beta} \epsilon^{-1}, \quad (51)$$

where  $\dot{x}_0 \equiv dx_0/dt$ . Finally, we can evaluate the right side of (50) using our estimates for  $\phi_1(\pm 1)$  in (39) and for  $u_c(z)$  as  $z \rightarrow \infty$ . This yields our main result of this section.

**Proposition: (Metastability)** *A metastable spike solution for (14), is represented by  $a(x, t) = a_E(x; x_0(t))$ , where  $a_E$  is defined in (15) and  $x_0(t)$  satisfies,*

$$\dot{x}_0(t) \sim \frac{2a^2\epsilon}{\hat{\beta}} \left[ e^{-2(1-x_0)/\epsilon} - e^{-2(1+x_0)/\epsilon} \right]. \quad (52)$$

Here  $a$  and  $\hat{\beta}$  are defined in (19) and (31), respectively.

For a given initial condition  $x_0(0) \in (-1, 1)$ , this ODE shows that the spike drifts towards the endpoint that is closest to the initial location  $x_0(0)$ . As a consistency check on our solvability condition  $D_1 = 0$ , we note from (31),

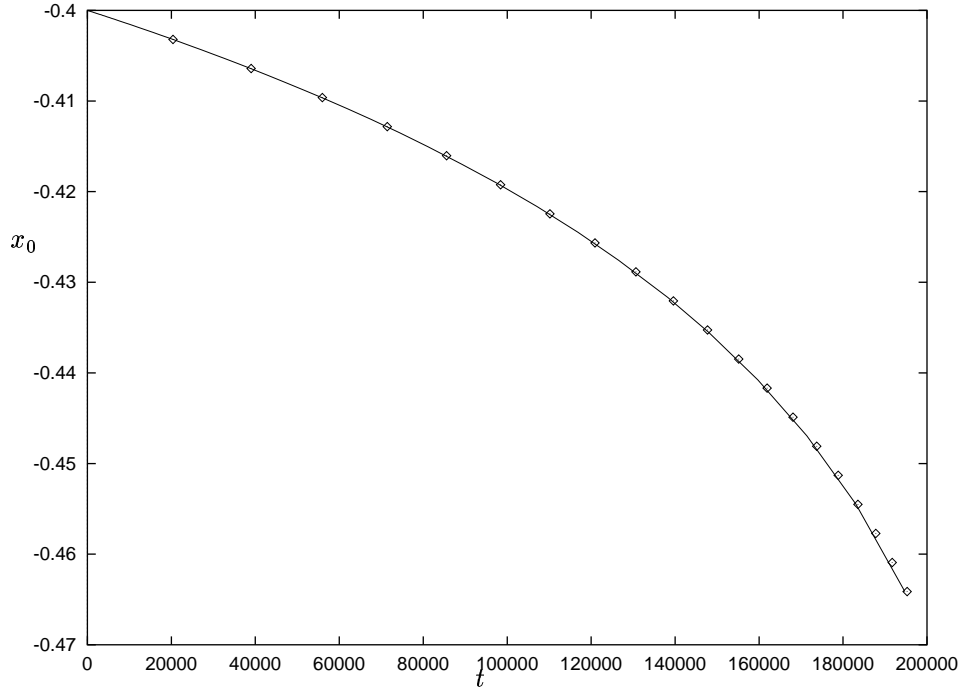


Figure 7:  $x_0$  versus  $t$  for  $\epsilon = .07$

(44), (51) and 52), that if the solvability condition were not imposed, then  $D_1\phi_1 = O(\epsilon^{-1/2})$ , which would violate our linearization assumption.

To verify the asymptotic result (52) we computed numerical solutions to (14) for various values of  $\epsilon$  for the parameter set  $(p, q, m, s) = (2, 1, 2, 0)$ . The computations were done by using a variable coefficient variable time step backward-differentiation (BDF) scheme to integrate in time (see [12] where a similar scheme is used). COLNEW was then used to solve the boundary value problem at each time step. At each time step the solution is calculated using a third and fourth order BDF scheme to estimate the error and determine the next maximum allowable time step. Comparisons of these results (solid curve) with a numerical integration of the asymptotic ODE (52) (dots) may be found in Fig. 5-7. In computing numerical solutions to (14) the initial condition  $a_E(x; x_0(0))$  was used for certain values of  $x_0(0)$  as can be seen from these figures.

### 3 A Spike in a Multi-Dimensional Domain

We now construct a quasi-equilibrium solution  $a_E$  for (13). This is done in a similar manner as in the one-dimensional case, except that the quasi-equilibrium solution will be radially symmetric about the center of the spike. Thus, we look for a steady-state solution to (13) in all of  $\mathbb{R}^N$  of the form

$$a = a_E(\mathbf{x}; \mathbf{x}_0) \equiv h^\gamma u_c(\epsilon^{-1}|\mathbf{x} - \mathbf{x}_0|), \quad \gamma = q/(p-1), \quad (53)$$

where  $\mathbf{x}_0$  is contained inside  $\Omega$  (i.e.  $\text{dist}(x_0, \partial\Omega) \gg O(\epsilon)$ ). The function  $u_c(\rho)$ , called the canonical spike solution, is a non-negative radially symmetric function, which decays exponentially as  $\rho \rightarrow \infty$ . It satisfies

$$u_c'' + \frac{N-1}{\rho} u_c' - u_c + u_c^p = 0, \quad \rho > 0, \quad (54a)$$

$$u_c'(0) = 0; \quad u_c(\rho) \sim a\rho^{(1-N)/2} e^{-\rho}, \quad \text{as } \rho \rightarrow \infty, \quad (54b)$$

where  $a > 0$  is some constant. In dimension  $N > 2$ , we require that  $p < p_c$ , where  $p_c$  is the critical Sobolev exponent for dimension  $N$ . In terms of this solution,  $h = h_E$ , where

$$h_E = \left( \frac{\epsilon^{-N}}{\mu|\Omega|} \int_{\Omega} u_c^m d\mathbf{x} \right)^{\frac{p-1}{(s+1)(p-1)-qm}}. \quad (55)$$

Here  $|\Omega|$  is the volume of  $\Omega$ . Since  $u_c$  is localized near  $\mathbf{x}_0$ , for  $\epsilon \rightarrow 0$  we get

$$h_E \sim \left( \frac{\Omega_N}{\mu|\Omega|} \int_0^\infty u_c^m \rho^{N-1} d\rho \right)^{\frac{p-1}{(s+1)(p-1)-qm}}, \quad (56)$$

where  $\Omega_N$  is the surface area of the unit  $N$ -dimensional sphere.

Recall that in the one-dimensional case and with  $p = 2$  we have the exact solution  $u_c(\rho) = \frac{3}{2} \text{sech}^2(\frac{\rho}{2})$ , and hence  $a = 6$ . To find numerical solutions for  $u_c(\rho)$  and for  $a$  in other dimensions, we will treat  $N$  as a real parameter, and use  $N$  (and  $p$  for  $p \neq 2$ ) as continuation parameters. We can use the far field asymptotic behavior (54b) to obtain the boundary condition  $u_c' = \frac{(1-N)}{2\rho} u_c$ , which we impose at some large value  $\rho = \rho_L$  in our numerical computations of (54). The computations are done using COLNEW. In Fig. 8 we plot the numerically computed solutions  $u_c(\rho)$  for  $N = 1, 2, 3$  when  $p = 2$ .

Since  $\text{dist}(x_0, \partial\Omega) \gg O(\epsilon)$ , we again note that  $a_E$  will satisfy the steady-state problem for (13a), but will fail to satisfy the no flux boundary condition (13c) by only exponentially small terms for any value of  $\mathbf{x}_0$  in the interior of  $\Omega$ . Thus, we expect that the spectrum of the eigenvalue problem associated with the linearization about  $a_E$  contains exponentially small eigenvalues.

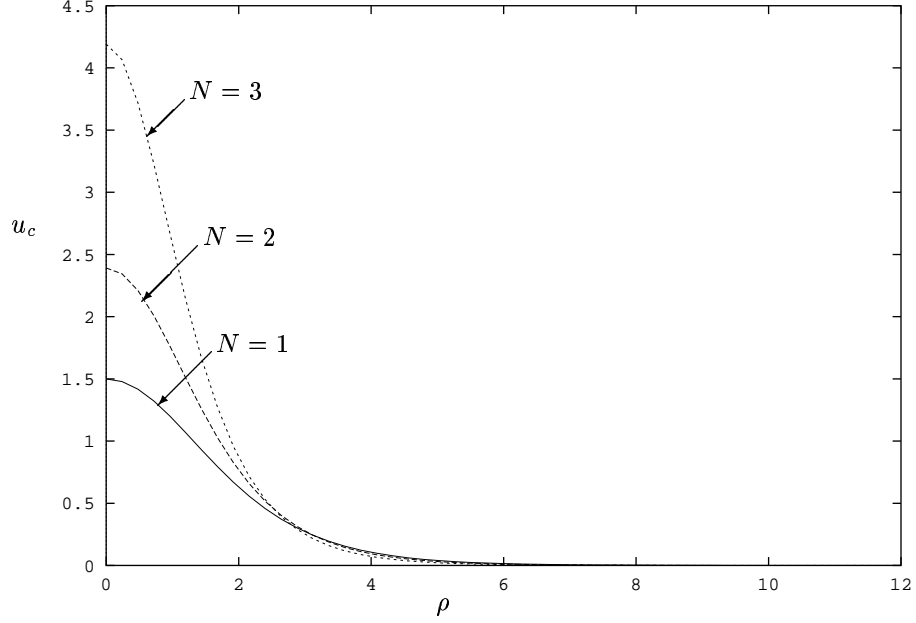


Figure 8: Numerical solution for  $u_c(\rho)$  when  $N = 1, 2, 3$  and  $p = 2$ .

### 3.1 The Nonlocal Eigenvalue Problem

Let  $\mathbf{x}_0 \in \Omega$  be fixed, and linearize (13) about  $a_E, h_E$ . We obtain the eigenvalue problem for this linearization by introducing  $\phi$  and  $\eta$  defined by

$$a(\mathbf{x}, t) = a_E(\mathbf{x}; \mathbf{x}_0) + e^{\lambda t} \phi(\mathbf{x}), \quad (57a)$$

$$h(t) = h_E + e^{\lambda t} \eta, \quad (57b)$$

where  $\phi \ll a_E$  and  $\eta \ll h$ . Substituting (57) into (13) we obtain, after a lengthy calculation, the following non-local eigenvalue problem;

$$L_\epsilon \phi \equiv \epsilon^2 \Delta \phi + (-1 + p u_c^{p-1}) \phi - \frac{m q \epsilon^{-N} u_c^p}{\beta_N \Omega_N (s+1)} \int_{\Omega} u_c^{m-1} \phi \, d\mathbf{x} = \lambda \phi, \quad \text{in } \Omega, \quad (58a)$$

$$\phi_n = 0 \quad \text{on } \partial\Omega. \quad (58b)$$

Here  $u_c = u_c[\epsilon^{-1}|\mathbf{x} - \mathbf{x}_0|]$ , and  $\beta_N$  is defined by

$$\beta_N = \int_0^\infty u_c^{m-1} \rho^{N-1} d\rho. \quad (59)$$

Since  $u_c$  is localized near  $\mathbf{x}_0$ , we will only seek eigenfunctions that are localized near  $\mathbf{x} = \mathbf{x}_0$ . These eigenfunctions are of the form

$$\tilde{\phi}(\mathbf{y}) = \phi(\mathbf{x}_0 + \epsilon\mathbf{y}), \quad \mathbf{y} = \epsilon^{-1}(\mathbf{x} - \mathbf{x}_0). \quad (60)$$

Therefore, we can replace  $\Omega$  by  $\mathbb{R}^n$  in (58a) and impose a decay condition for  $\tilde{\phi}$  as  $|\mathbf{y}| \rightarrow \infty$ . This gives us the non-local eigenvalue problem for the infinite domain

$$\hat{L}_\epsilon \tilde{\phi} \equiv \Delta_{\mathbf{y}} \tilde{\phi} + (-1 + pu_c^{p-1}) \tilde{\phi} - \frac{mqu_c^p}{\beta_N \Omega_N (s+1)} \int_{\mathbb{R}^N} u_c^{m-1} \tilde{\phi} d\mathbf{y} = \tilde{\lambda} \tilde{\phi}, \quad \text{in } \mathbb{R}^N, \quad (61a)$$

$$\tilde{\phi} \rightarrow 0 \quad \text{as } |\mathbf{y}| \rightarrow \infty. \quad (61b)$$

In this problem  $u_c = u_c(|\mathbf{y}|)$ . If, in addition, we consider an eigenfunction that is radially symmetric (i. e.  $\tilde{\phi} = \tilde{\phi}(\rho)$ , where  $\rho = |\mathbf{y}|$ ), then (61) reduces to

$$\tilde{L}_\epsilon \tilde{\phi} \equiv \Delta_\rho \tilde{\phi} + (-1 + pu_c^{p-1}) \tilde{\phi} - \frac{mqu_c^p}{\beta_N (s+1)} \int_0^\infty u_c^{m-1} \tilde{\phi} \rho^{N-1} d\rho = \tilde{\lambda} \tilde{\phi}, \quad \rho > 0, \quad (62a)$$

$$\tilde{\phi} \rightarrow 0 \quad \text{as } \rho \rightarrow \infty, \quad (62b)$$

where  $\Delta_\rho \tilde{\phi} \equiv \tilde{\phi}'' + (N-1)\rho^{-1}\tilde{\phi}'$ .

We now analyze the spectrum of these eigenvalue problems. We first note that, for each  $i = 1, \dots, N$ , the function  $\tilde{\phi}_i = \partial_{y_i} u_c(|\mathbf{y}|)$  satisfies (61). Here  $y_i$  is the  $i^{\text{th}}$  coordinate of  $\mathbf{y}$ . This follows from the combined effects of translation invariance and the vanishing of the integral in (61) by symmetry considerations. Thus, (61) has a zero eigenvalue of multiplicity  $N$  with corresponding eigenfunctions  $\tilde{\phi}_i = \partial_{y_i} u_c(|\mathbf{y}|)$  for  $i = 1, \dots, N$ . Each of these eigenfunctions has one nodal line. These eigenpairs will be perturbed by only exponentially small terms as a result of the finite domain. Hence, there are  $N$  eigenvalues of (58) that are exponentially small, and they are estimated below. The goal is to determine whether these are the principal eigenvalues of (58).

We claim that these are not the principal eigenvalues for (58) when the non-local term in (58) is absent. To see this, suppose that the non-local term in (58), (61) and (62) is absent. The corresponding eigenvalue problems are then local and self-adjoint, and several key properties follow. In particular, since  $\tilde{\phi}_i = \partial_{y_i} u_c(|\mathbf{y}|)$  is an eigenfunction of (61) with a zero eigenvalue and has one-nodal line, the local eigenvalue problem must have a simple, positive eigenvalue, which is independent of  $\epsilon$ . The corresponding positive, radially symmetric, eigenfunction satisfies the local version of (62). The effect of the finite domain in (58) is to perturb this eigenvalue by only exponentially small

terms. Thus, when the non-local term is absent no metastable behavior can occur.

The effect of the non-local term will be to ensure that the exponentially small eigenvalues are the principal eigenvalues for the non-local eigenvalue problem (58). Thus, the quasi-equilibrium solution will be metastable if we can show that the principal eigenvalue of (62) has a negative real part. To do so, we compute the eigenvalues and eigenfunctions of the radially symmetric problem (62), where a continuation parameter  $\delta$ , with  $0 \leq \delta \leq 1$ , multiplies the nonlocal term

$$L_\delta \tilde{\phi} \equiv \Delta_\rho \tilde{\phi} + (-1 + pu_c^{p-1})\tilde{\phi} - \delta \frac{mq u_c^p}{\beta_N (s+1)} \int_0^\infty u_c^{m-1} \tilde{\phi} \rho^{N-1} d\rho = \lambda \tilde{\phi}, \quad \rho > 0, \quad (63a)$$

$$\tilde{\phi} \rightarrow 0 \quad \text{as} \quad \rho \rightarrow \infty. \quad (63b)$$

We compute the eigenvalues of this problem as a function of  $\delta$ , and in particular track the first eigenvalue  $\lambda_0(\delta)$ . We will show that the positive principal eigenvalue  $\lambda_0(0)$ , which occurs when the non-local term is absent, will cross through zero into the left half plane as  $\delta$  increases. Thus, we must show that the first eigenvalue  $\lambda_0(\delta)$  has a negative real part when  $\delta = 1$ .

For the parameter set ( $p = 2, q = 1, m = 2, s = 0$ ), in Fig. 9 and Fig. 10 we plot the first two eigenvalues  $\lambda_0(\delta)$  and  $\lambda_{N+1}(\delta)$  of (63) as a function of  $\delta$  for  $N = 2$  and  $N = 3$ , respectively. Here  $\lambda_{N+1}$  is the first eigenvalue in the sequence for (61) following the zero  $\lambda_i, i = 1, \dots, N$ . These computations were done using COLNEW. These plots clearly indicate that  $\lambda_0(\delta)$  crosses through 0 before  $\delta = 1$ . At some value of  $\delta$ ,  $\lambda_0$  and  $\lambda_{N+1}$  collide and become complex. To track the eigenvalues past the point where they become complex, we use the same technique as in the one-dimensional case. The differential operator is approximated by a matrix and the eigenvalues of the matrix are then approximations of the eigenvalues of the differential operator. Using this numerical procedure, we give numerical values for the real and imaginary part of  $\lambda_0(\delta)$  in Table 2. This table shows that the real part of  $\lambda_0$  is negative when  $\delta = 1$ . Similar computations, with similar conclusions, can be performed for other values of  $p, q, m$  and  $s$ .

### 3.2 An Exponentially Small Eigenvalue

We will now use a boundary layer analysis to construct a composite approximation to the eigenfunctions corresponding to the exponentially small eigenvalues of (58). The corresponding eigenfunctions are well approximated by  $\partial_{x_i} u_c$ , for  $i = 1, \dots, N$  in the interior of the domain and each of these eigenfunctions has a boundary layer correction term near  $\partial\Omega$  in order to satisfy the no-flux boundary condition on  $\partial\Omega$ . In order to resolve the boundary layer we must define a local coordinate system. Let  $\hat{\eta}$  represent the distance from a point in  $\Omega$  to  $\partial\Omega$ , where  $\hat{\eta} < 0$  corresponds to the interior of  $\Omega$ . Let  $\zeta$  correspond to the other  $N - 1$  orthogonal coordinates. To localize the region near  $\partial\Omega$ , we let  $\eta = \epsilon^{-1} \hat{\eta}$ . The

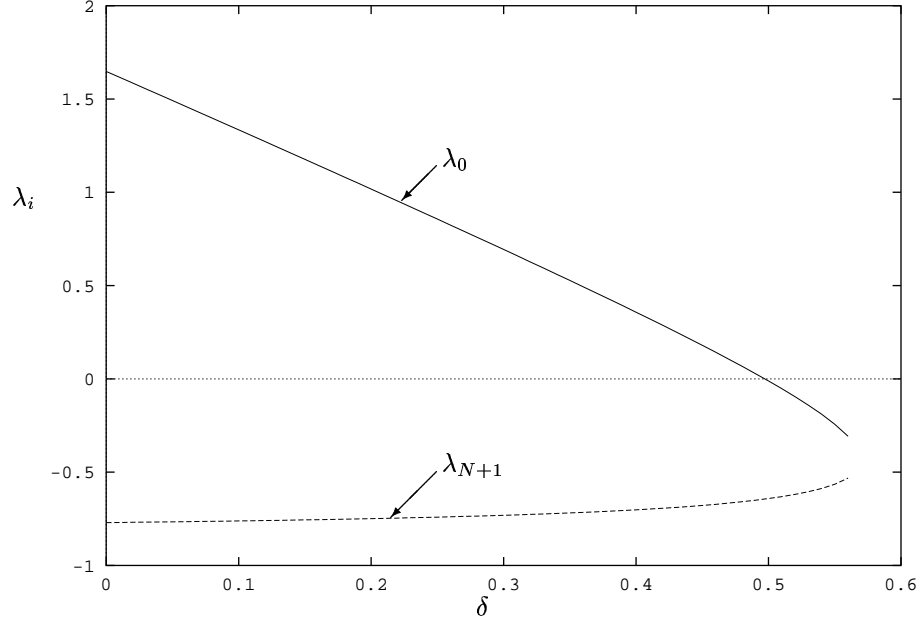


Figure 9:  $\lambda_0(\delta)$  and  $\lambda_{N+1}(\delta)$  versus  $\delta$  in  $\mathbb{R}^2$  for the parameter set  $(p = 2, q = 1, m = 2, s = 0)$ .

eigenfunction on the finite domain can then be approximated by,

$$\phi_i = C_i \left( \partial_{x_i} u_c (\epsilon^{-1} |\mathbf{x} - \mathbf{x}_0|) + \hat{\phi}_i \right), \quad (64)$$

where  $C_i$  is a normalization constant and  $\hat{\phi}_i$  is a boundary layer correction term. Using the fact that  $u_c$  is exponentially small near  $\partial\Omega$  we get the following boundary layer problem

$$\partial_{\eta\eta} \hat{\phi}_i - \hat{\phi}_i = 0, \quad \eta < 0, \quad (65)$$

$$\partial_{\eta} \hat{\phi}_i = \underbrace{-\epsilon \partial_{\hat{\eta}} (\partial_{x_i} u_c)|_{\eta=0}}_{\text{a function of } \zeta}, \quad \text{on } \eta = 0, \quad (66)$$

$$\hat{\phi}_i \rightarrow 0 \quad \text{as } \eta \rightarrow -\infty. \quad (67)$$

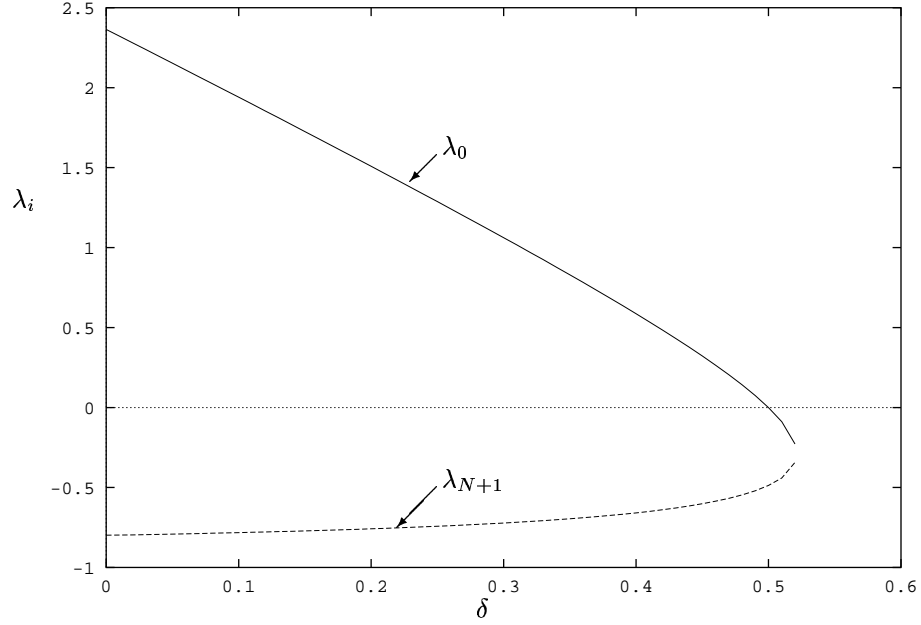


Figure 10:  $\lambda_0(\delta)$  and  $\lambda_{N+1}(\delta)$  versus  $\delta$  in  $\mathbb{R}^3$  for the parameter set ( $p = 2, q = 1, m = 2, s = 0$ ).

We require that  $\hat{\phi}_i \rightarrow 0$  as  $\eta \rightarrow -\infty$  to match to the outer solution. Then, the solution for  $\hat{\phi}_i$  is

$$\hat{\phi}_i = \epsilon g_i(\zeta) e^\eta, \quad \text{where} \quad g_i(\zeta) \equiv -\partial_{\hat{\eta}}(\partial_{x_i} u_c)|_{\eta=0} \quad (68)$$

Thus, the composite asymptotic solution for the eigenfunction is

$$\phi_i = C_i \left[ \partial_{x_i} u_c + \epsilon g_i(\zeta) e^{\hat{\eta}/\epsilon} \right], \quad i = 1 \dots, N. \quad (69)$$

Below we need an estimate for  $\phi_i$  on  $\partial\Omega$ . To do so we need to calculate  $g_i$ . Let  $x_{0i}$  represent the  $i^{\text{th}}$  coordinate of  $\mathbf{x}_0$ . So, setting  $r = |\mathbf{x} - \mathbf{x}_0|$ , we apply the chain rule, which gives

$$g_i \sim -\frac{(x_i - x_{0i})}{\epsilon^2 r} [u_c''(r/\epsilon) \mathbf{r} \cdot \mathbf{n}], \quad (70)$$

$\delta$	$\lambda_0$ in $\mathbb{R}^2$	$\lambda_0$ in $\mathbb{R}^3$
0.00000	1.6388	2.3703
0.05000	1.4814	2.1588
0.10000	1.3231	1.9456
0.15000	1.1638	1.7304
0.20000	1.0030	1.5125
0.25000	0.84032	1.2910
0.30000	0.67516	1.0646
0.35000	0.50641	0.83098
0.40000	0.33218	0.58554
0.45000	0.14857	0.31741
0.50000	-.055026	-.019898
0.55000	-.37526	-.33843 + 0.29744i
0.60000	-.48239 + 0.24569i	-.44368 + 0.45028i
0.65000	-.56115 + 0.33165i	-.54978 + 0.54508i
0.70000	-.64059 + 0.38475i	-.65696 + 0.60964i
0.75000	-.72097 + 0.41770i	-.76550 + 0.65310i
0.80000	-.80268 + 0.43510i	-.87584 + 0.67970i
0.85000	-.88640 + 0.43886i	-.98857 + 0.69170i
0.90000	-.97333 + 0.42959i	-1.1045 + 0.69037i
0.95000	-1.0657 + 0.40726i	-1.2249 + 0.67652i
1.00000	-1.1678 + 0.37248i	-1.3513 + 0.65089i

Table 2:  $\delta$  and  $\lambda_0$  in  $\mathbb{R}^2$  and  $\mathbb{R}^3$  for the case of  $(p = 2, q = 1, m = 2, s = 0)$ .

where  $\mathbf{n}$  is the outward unit normal to  $\Omega$ . Since  $u_c(\rho) \sim a\rho^{(1-N)/2}e^{-\rho}$  as  $\rho \rightarrow \infty$  we get that,

$$g_i \sim -a\epsilon^{(N-5)/2}(x_i - x_{0i})r^{-(1+N)/2}e^{-r/\epsilon}\mathbf{r} \cdot \mathbf{n}, \quad \text{on } \partial\Omega. \quad (71)$$

Combining (69) with (71), we get an asymptotic approximation for  $\phi_i$  on  $\partial\Omega$ ,

$$\phi_i \sim -C_i a\epsilon^{(N-3)/2}a(x_i - x_{0i})r^{-(1+N)/2}e^{-r/\epsilon}(1 + \mathbf{r} \cdot \mathbf{n}), \quad \text{on } \partial\Omega. \quad (72)$$

In order to complete our asymptotic estimate of the exponentially small eigenvalues, we apply Green's identity to  $\phi_i$  and  $\partial_{x_i}u_c$  to get the following relationship:

$$\lambda_i(\partial_{x_i}u_c, \phi_i) = -\epsilon^2 \int_{\partial\Omega} \phi_i \partial_n(\partial_{x_i}u_c) dS + (L_\epsilon^*[\partial_{x_i}u_c], \phi_i). \quad (73)$$

Here  $L_\epsilon^*$  is the adjoint of  $L_\epsilon$ ,

$$L_\epsilon^*v \equiv \epsilon^2 \Delta v - v + u_c^{p-1}v - \frac{mq\epsilon^{-N}u_c^{m-1}}{\beta_N \Omega_N(s+1)} \int_{\Omega} u_c^p dx. \quad (74)$$

We will now estimate each term in (73). Since  $\partial_{x_i} u_c$  is an exact solution to the local problem, we have that,

$$L_\epsilon^* (\partial_{x_i} u_c) = -\frac{mq\epsilon^{-N} u_c^{m-1}}{\beta_N \Omega_N (s+1)} \int_\Omega u_c^p \partial_{x_i} u_c \, d\mathbf{x}. \quad (75)$$

Next, since  $u_c$  is radially symmetric and localized to a small region in the interior of  $\Omega$ , it is clear that  $\int_\Omega u_c^p \partial_{x_i} u_c \, d\mathbf{x} \sim \int_\Omega u_c^p \partial_{x_j} u_c \, d\mathbf{x}$ , as  $\epsilon \rightarrow 0 \, \forall i, j = 1 \dots N$ . Thus, we may write the expression above as,

$$L_\epsilon^* (\partial_{x_i} u_c) \sim -\frac{mq\epsilon^{-N} u_c^{m-1}}{N\beta_N \Omega_N (s+1)} \int_\Omega \sum_{i=1}^N u_c^p \partial_{x_i} u_c \, d\mathbf{x}. \quad (76)$$

An application of the Divergence Theorem results in,

$$L_\epsilon^* (\partial_{x_i} u_c) \sim -\frac{mq\epsilon^{-N} u_c^{m-1}}{N\beta_N \Omega_N (s+1)} \int_{\partial\Omega} \left( \frac{u_c^{p+1}}{p+1} \right) dS. \quad (77)$$

On the boundary of  $\Omega$ ,  $u_c [\epsilon^{-1} |\mathbf{x} - \mathbf{x}_0|] \sim a\epsilon^{(N-1)/2} r^{(1-N)/2} e^{-\epsilon^{-1} |\mathbf{x} - \mathbf{x}_0|}$ . Therefore, the integral in (77) will be exponentially small. We then estimate the integral in (77) to get the following bound:

$$|L_\epsilon^* (\partial_{x_i} u_c)| < D\epsilon^{-N} |\partial\Omega| u_c^{m-1} \epsilon^{(N-1)(p+1)/2} \rho_0^{(1-N)(p+1)/2} e^{-\epsilon^{-1} (p+1)\rho_0}, \quad (78)$$

where

$$D = \frac{mqa^{p+1}}{N\beta_N \Omega_N (s+1)(p+1)}. \quad (79)$$

Here  $\rho_0 = \text{dist}(\mathbf{x}_0, \partial\Omega)$ . Therefore, with  $\phi_i \sim C_i \partial_{x_i} u_c$ , we have

$$\begin{aligned} |(L_\epsilon^* (\partial_{x_i} u_c), \phi_i)| &< DC_i \epsilon^{-N} |\partial\Omega| \epsilon^{(N-1)(p+1)/2} \\ &\times \rho_0^{(1-N)(p+1)/2} e^{-\epsilon^{-1} (p+1)\rho_0} \int_\Omega u_c^{m-1} \partial_{x_i} u_c \, d\mathbf{x}. \end{aligned} \quad (80)$$

A similar procedure shows that

$$\begin{aligned} |(L_\epsilon^* \partial_{x_i} u_c, \phi_i)| &< \frac{a^m |\partial\Omega|^2 DC_i \epsilon^{-N}}{mN} \\ &\times \epsilon^{(N-1)(p+m+1)/2} \rho_0^{-(N-1)(p+m+1)/2} e^{-\epsilon^{-1} \rho_0 (p+m+1)}. \end{aligned} \quad (81)$$

Therefore, we conclude that

$$|(L_\epsilon^* \partial_{x_i} u_c, \phi_i)| = 0 \left( \epsilon^b e^{-\epsilon^{-1} \rho_0 (p+m+1)} \right), \quad (82)$$

for some  $b$ . We will show that this term is exponentially smaller than the first term on the right side of (73), and therefore, we can ignore it.

Now we estimate the left hand side of (73). Since  $\phi_i$  and  $\partial_{x_i} u_c$  are exponentially small outside of a neighborhood of  $\mathbf{x} = \mathbf{x}_0$ , this inner product is dominated by the contribution from  $\mathbf{x} = \mathbf{x}_0$ . Using a Laplace-type approximation, we can approximate the inner product to get

$$(\partial_{x_i} u_c, \phi_i) \sim \frac{C_i}{\epsilon^2} \int_{\Omega} [u'_c(r/\epsilon)]^2 \left( \frac{x_i - x_{0i}}{r} \right)^2 d\mathbf{x} \sim \frac{C_i \epsilon^{N-2}}{N} \int_{\mathbb{R}^N} [u'_c(\rho)]^2 \rho^{N-1} d\rho d\theta, \quad (83)$$

where  $\theta$  represents the  $N - 1$  angular co-ordinates. Since the integrand is independent of  $\theta$ ,

$$(\partial_{x_i} u_c, \phi_i) \sim C_i \epsilon^{N-2} \Omega_N \hat{\beta}_N / N, \quad \text{where} \quad \hat{\beta}_N \equiv \int_0^\infty [u'_c(\rho)]^2 \rho^{N-1} d\rho. \quad (84)$$

Here  $\Omega_N$  is the surface area of the  $N$ -dimensional unit sphere. Then we determine  $C_i$  by using the normalization relation  $\int_{\Omega} \phi_i^2 d\mathbf{x} = 1$  to obtain,

$$C_i = \left( \frac{N}{\hat{\beta}_N \Omega_N} \right)^{1/2} \epsilon^{(2-N)/2}. \quad (85)$$

Finally, we get our asymptotic estimate of  $\lambda_i$  by substituting (84) and (72) into (73), and using the estimate  $\partial_n(\partial_{x_i} u_c) \sim a \epsilon^{(N-5)/2} r^{-(N+1)/2} e^{-r/\epsilon}$ , on  $\partial\Omega$ . In this way, we get

$$\lambda_i \sim \frac{a^2 N}{\hat{\beta}_N \Omega_n} \int_{\partial\Omega} (x_i - x_{0i})^2 r^{-(1+N)} e^{-2r/\epsilon} (\mathbf{r} \cdot \mathbf{n})(1 + \mathbf{r} \cdot \mathbf{n}) dS, \quad (86)$$

where  $\mathbf{r} = (\mathbf{x} - \mathbf{x}_0)/r$  and  $r = |\mathbf{x} - \mathbf{x}_0|$ , with  $\mathbf{x} \in \partial\Omega$ . As a consistency check we observe by comparing the asymptotic orders of the two terms on the right side of (73) that the second term is asymptotically negligible compared to the first term, since the exponents satisfy  $p + m + 1 > 1$ .

The surface integral in (86) can be evaluated asymptotically by using a multi-dimensional Laplace technique. Assume that there exists a unique point  $\mathbf{x}_m \in \partial\Omega$  where  $r_m = \text{dist}(\mathbf{x}_0, \partial\Omega)$  is minimized. If we parameterize the boundary near  $\zeta_m$  (where  $\mathbf{x}(\zeta_m) = \mathbf{x}_m$ ) such that each  $\zeta_i$  corresponds to arclength along one of the principal directions through  $\zeta_m$ , then for any smooth  $F(r)$ , we have (see [15]),

$$\int_{\partial\Omega} r^{1-N} F(r) e^{-2r/\epsilon} dS = \left( \frac{\pi\epsilon}{r_m} \right)^{(N-1)/2} F(r_m) H(r_m) e^{-2r_m/\epsilon}, \quad (87)$$

where

$$H(r_m) \equiv (1 - r_m/R_1)^{-1/2} (1 - r_m/R_2)^{-1/2} \dots (1 - r_m/R_{N-1})^{-1/2}. \quad (88)$$

Here  $R_j > 0$ , for  $j = 1, \dots, N - 1$  are the principal radii of curvature of  $\partial\Omega$  at  $\mathbf{x}_m$ . This result assumes that the non-degeneracy condition  $R_j > r_m$ ,  $j =$

$1, \dots, N-1$  holds. In this way, we obtain the following explicit asymptotic estimate for the exponentially small eigenvalue,

$$\lambda_i \sim \frac{2a^2 N}{\hat{\beta}_N \Omega_N} \left( \frac{\pi \epsilon}{r_m} \right)^{(N-1)/2} \left( \frac{\mathbf{r}_m \cdot \mathbf{e}_i}{r_m} \right)^2 H(r_m) e^{-2r_m/\epsilon}, \quad (89)$$

where  $\mathbf{e}_i$  is the standard unit basis vector in the  $i^{\text{th}}$  direction and  $\mathbf{r}_m \equiv (x_m - x_0)/r_m$ .

### 3.3 The Slow Motion of the Spike

Now we derive an ODE characterizing the metastable spike dynamics. We first linearize (13) about a moving spike by writing,

$$a(\mathbf{x}, t) = a_E(\mathbf{x}; \mathbf{x}_0(t)) + w(x, t), \quad (90)$$

where  $a_E(\mathbf{x}; \mathbf{x}_0)$  is defined in (53). Since, (58) does not have an  $O(1)$  positive eigenvalue, we may assume that  $w \ll a_E$ ,  $w_t \ll \partial_t a_E$  uniformly in time. Substituting (90) into (13), we obtain

$$L_\epsilon w = \partial_t a_E, \quad \text{in } \Omega, \quad (91a)$$

$$\partial_n w = -\partial_n a_E, \quad \text{on } \partial\Omega. \quad (91b)$$

Next, we expand  $w$  in terms of the eigenfunctions  $\phi_i$  of  $L_\epsilon$  as

$$w = \sum_{i=1}^{\infty} D_i(t) \phi_i. \quad (92)$$

We assume that the eigenfunctions form a complete set. However, this is not required for the construction of the solvability condition as the key requirement is that  $w$  is orthogonal to the eigenspace of  $L_\epsilon^*$  associated with the exponentially small eigenvalues. Let  $\phi_i^*$  be the  $i^{\text{th}}$  eigenfunction of  $L_\epsilon^*$ . Then, since  $(\phi_i, \phi_j^*) = \delta_{ij}$ , we integrate by parts to show that

$$D_i(t) = (w, \phi_i^*) = \frac{1}{\lambda_i^*} \left[ (L_\epsilon w, \phi_i^*) - \epsilon^2 \int_{\partial\Omega} w_n \phi_i^* dS \right], \quad (93)$$

where  $L_\epsilon^* \phi_i^* = \lambda_i^* \phi_i^*$ . Using (91), we have

$$D_i(t) = \frac{1}{\lambda_i^*} \left[ (\partial_t a_E, \phi_i^*) + \epsilon^2 \int_{\partial\Omega} \partial_n a_E \phi_i^* dS \right]. \quad (94)$$

As seen in (73)-(82), the nonlocal term in the eigenvalue problem  $L_\epsilon \phi = \lambda \phi$  is insignificant when  $\epsilon \ll 1$  in the asymptotic estimation of the eigenspace associated with the exponentially small eigenvalues of  $L_\epsilon$ . Therefore, for  $i = 1, \dots, N$ , we can replace  $\phi_i^*$  and  $\lambda_i^*$  by  $\phi_i$  and  $\lambda_i$  in (94), where  $\phi_i$  and  $\lambda_i$  are given in (69) and (89), respectively.

Since  $\lambda_i \rightarrow 0$  exponentially as  $\epsilon \rightarrow 0$ , for  $i = 1, \dots, N$ , we must impose the limiting solvability conditions that  $D_i = 0$ , for  $i = 1, \dots, N$ . This projection step yields the following implicit differential equation for  $\mathbf{x}_0(t)$ :

$$(\partial_t a_E, \phi_i) = -\epsilon^2 \int_{\partial\Omega} \partial_n a_E \phi_i dS. \quad (95)$$

The dominant contribution to the left side of (95) arises from the region near  $\mathbf{x}_0$ , and we calculate

$$(\partial_t a_E, \phi_i) \sim -\frac{C_i h_E^\gamma}{N} \dot{x}_{0i} \Omega_N \hat{\beta}_N \epsilon^{N-2}. \quad (96)$$

Finally, we can evaluate the right side of (95) using our estimates for  $\phi_i$  on  $\partial\Omega$  in (72) and for  $u_c(\rho)$  as  $\rho \rightarrow \infty$ . This yields the main result of this section.

**Proposition: (Metastability)** *A metastable spike solution for (13), is represented by  $a(\mathbf{x}, t) = a_E(\mathbf{x}; \mathbf{x}_0(t))$ , where  $a_E$  is defined in (53) and  $\mathbf{x}_0(t)$  satisfies,*

$$\dot{\mathbf{x}}_0 \sim \frac{\epsilon N a^2}{\hat{\beta}_N \Omega_N} \int_{\partial\Omega} \hat{\mathbf{r}} r^{1-N} e^{-2r/\epsilon} (1 + \hat{\mathbf{r}} \cdot \mathbf{n}) \hat{\mathbf{r}} \cdot \mathbf{n} dS. \quad (97)$$

Here  $\hat{\mathbf{r}} = (\mathbf{x} - \mathbf{x}_0)r^{-1}$ ,  $r = |\mathbf{x} - \mathbf{x}_0|$ ,  $\mathbf{x} \in \partial\Omega$ , and  $\mathbf{n}$  is the unit outward normal to  $\partial\Omega$ . In addition,  $a$  and  $\hat{\beta}_N$  are defined in (54b) and (84), respectively.

There are a few corollaries that follow from this result.

**Corollary 1: (Equilibrium)** *An equilibrium solution for (13), is represented by  $a(\mathbf{x}, t) = a_E(\mathbf{x}; \mathbf{x}_{0e})$ , where  $\mathbf{x}_{0e}$  is a root of  $I(\mathbf{x}_0)$ , where*

$$I(\mathbf{x}_0) \equiv \int_{\partial\Omega} \hat{\mathbf{r}} r^{1-N} e^{-2r/\epsilon} (1 + \hat{\mathbf{r}} \cdot \mathbf{n}) \hat{\mathbf{r}} \cdot \mathbf{n} dS \quad (98)$$

It was shown in [15] that for a strictly convex domain  $\mathbf{x}_{0e}$  is unique and is centered at an  $O(\epsilon)$  distance from the center of the uniquely determined largest inscribed sphere for  $\Omega$ . This equilibrium solution is unstable.

Assuming that there is a unique point  $\mathbf{x}_m \in \partial\Omega$  closest to the initial center  $\mathbf{x}_0(0)$  of the spike, we can evaluate the surface integral in (97) using Laplace's method to get the following explicit result:

**Corollary 2: (Explicit Motion)** *Let  $\mathbf{x}_m$  be the point on  $\partial\Omega$  closest to  $\mathbf{x}_0(0)$ . Then, for  $t > 0$ , the spike moves in the direction of  $\mathbf{x}_m$  and the distance  $r_m(t) = |\mathbf{x}_m - \mathbf{x}_0(t)|$ , satisfies the first order nonlinear differential equation*

$$\dot{r}_m = -\xi r_m \left( \frac{\epsilon}{r_m} \right)^{(N+1)/2} H(r_m) e^{-2r_m/\epsilon}, \quad (99)$$

where

$$\xi \equiv \frac{2N a^2}{\Omega_N \hat{\beta}_N} \pi^{(N-1)/2}. \quad (100)$$

Here  $\hat{\beta}_N$  is defined in (84) and  $H(r_m)$  is determined in the terms of the principal radii of curvature of  $\partial\Omega$  in (88).

This result is valid up until the spike approaches to within an  $O(\epsilon)$  distance of  $\mathbf{x}_m$ . If the initial condition for (99) is  $r_m(0) = r_0$ , then the time  $T$  needed for  $r_m(T) = 0$ , is readily found to be

$$T \sim \frac{\epsilon^{(1-N)/2} r_0^{(N-1)/2}}{2H(r_0)\xi} e^{2r_0/\epsilon}. \quad (101)$$

Once the spike reaches the boundary, it moves in the direction of increasing mean curvature until it reaches an equilibrium point where the mean curvature of the boundary has a local maximum (see [2]). The existence of such equilibrium solutions, where the spike is located at these special points on the boundary, is demonstrated rigorously in [5], [9].

## 4 Conclusions

Although this analysis was carried out on the Gierer Meinhardt system, the results may be generalized to a much wider class of non-local reaction diffusion equations that have localized spike solutions. The key feature of the analysis lies in determining if the exponentially small eigenvalue associated with the linearization around the spike solution is in fact the principal eigenvalue of this linearization. In a scalar reaction diffusion model, with no non-local effects, that is capable of supporting spike-type solutions, it has been demonstrated that there will always be one eigenvalue bounded above from zero as well as an exponentially small eigenvalue[15], thus eliminating the possibility of metastability. For the non-local system, we have established that the non-local term may push this positive eigenvalue into the left half plane, thus making the exponentially small eigenvalue the principle eigenvalue. In the case of the limiting form of the Gierer Meinhardt equations analyzed above, this has been confirmed using numerical techniques that employ a homotopy between the local and non-local operators. This usually involves extensive computations. There are several similar systems that are presently under investigation, which may lead to more general results.

There remains many interesting questions for the full Gierer Meinhardt model. Numerical studies show that the dynamics in the case of large, but finite,  $D_h$  is very different in character from the case of infinite  $D_h$ . As  $D_h$  is decreased from infinity, a single spike centered at  $x_0 = 0$  will become stable. As  $D_h$  is decreased further the system appears to admit stable multiple spike solutions. The spike dynamics is not metastable in this case.

## References

- [1] U. Ascher, R. Christiansen, and R. Russell. Collocation software for boundary value ode's. *Math. Comp.*, 33:659–679, 1979.

- [2] D.Iron and M.J. Ward. The motion of boundary spikes for the Gierer-Meinhardt model. in preparation, 1998.
- [3] P. Freitas. A nonlocal Sturm-Liouville eigenvalue problem. *Proc. Roy. Soc. Edinburgh*, 12A:169–188, 1994.
- [4] A. Gierer and H. Meinhardt. A theory of biological pattern formation. *Kybernetik*, 12:30–39, 1972.
- [5] C. Gui. Multi-peak solutions for a semilinear Neumann problem. *Duke Mathematical Journal*, Vol.84(No.3):739–769, 1996.
- [6] David M. Holloway. *Reaction-diffusion theory of localized structures with application to vertebrate organogenesis*. PhD thesis, University of British Columbia, March 1995.
- [7] J. P. Keener. Activators and inhibitors in pattern formation. *Stud. Appl. Math*, 59:1–23, 1978.
- [8] G. L. Lamb. *Elements of Soliton Theory*. Wiley Interscience, 1980.
- [9] W.M. Ni and I. Takagi. On the shape of least-energy solutions to a semi-linear Neumann problem. *Comm. Pure Appl. Math*, XLIV:819–851, 1991.
- [10] W.M. Ni and I. Takagi. Point-condensation generated by a reaction-diffusion system in axially symmetric domains. *Japan J. Indust. Appl. Math*, 12(2):327–365, 1995.
- [11] Y. Nishiura. Global structure of bifurcating solutions of some reaction-diffusion systems. *SIAM J. Math. Anal.*, 13(4):555–593, 1982.
- [12] X. Sun and M.J. Ward. Metastability for a generalized burgers equation with applications to propagating flame fronts. to appear, *European J. Appl. Math.*, 1998.
- [13] I. Takagi. Point-condensation for a reaction-diffusion system. *J. Differential Equations*, 61:208–249, 1986.
- [14] A. Turing. The chemical basis of morphogenesis. *Phil. Trans. Roy. Soc. B*, 32, 1952.
- [15] M.J. Ward. An asymptotic analysis of localized solutions for some reaction-diffusion models in multi-dimensional domains. *Stud. Appl. Math*, 97(2):103–126, 1996.
- [16] M.J. Ward. Metastable bubble solutions for the Allen - Cahn equation with mass conservation. *SIAM J. Appl. Math.*, 5(1247-1279), 1996.
- [17] M.J. Ward. *Boundaries, Interfaces and Transitions*, chapter Dynamical metastability and singular perturbations, pages 237–263. CRM Proc. Lecture Notes, vol. 13, AMS, Providence, R.I., 1998.